J Mater Sci (2011) 46:7074–7081
DOI 10.1007/s10853-011-5502-z

SIZE DEPENDENT EFFECTS

Nanomodified NiFe- and NiFeP-carbon felt as anode electrocatalysts in yeast-biofuel cell

Yolina Hubenova · Rashko Rashkov · Vasil Buchvarov · Sofia Babanova · Mario Mitov

Received: 20 December 2010 / Accepted: 22 March 2011 / Published online: 8 April 2011

Abstract The improvement of the electron transfer from the microorganisms to the anode is considered to be one of the most important factors for increasing the biofuel cell efficiency. In our recent study, a significant improvement of the yeast-biofuel cell output was achieved by application of Ni-modified carbon felt anodes. In this study, the electrocatalytic properties of new nanomodified carbon materials were investigated. Nickel–iron and nickel–iron–phosphorous nanostructures were electrodeposited on carbon felt by means of pulse plating technique. The produced materials were analyzed for cytotoxicity and applied as anodes in a double-chamber mediatorless yeast-biofuel cell. The use of all modified electrodes resulted in increase of the biofuel cell outputs in comparison with those obtained with non-modified carbon felt; however, higher maximum power density values, exceeding up to 5-folds that of the control, have been achieved with NiFeP-carbon felt anodes. The observed electrocatalytic effects were connected with the particular elemental content, size distribution, and morphology of modified materials as well as with a hypothesis for switching on adaptive mechanisms as a response to Ni and Fe presence, resulting in facilitated electron transfer across the cell membrane.

Abbreviations

MFC	Microbial fuel cell
SEM	Scanning electron microscopy
EDX	Energy dispersion X-ray
CV	Cyclic voltammetry
OD600	Optical density at 600 nm
NME	Non-modified electrode
$NiFe_{(g.)}$	Galvanostatically modified NiFe-carbon felt
$NiFe_{(p.)}$	Potentiostatically modified NiFe-carbon felt
$NiFeP_{(g.)}$	Galvanostatically modified NiFeP-carbon felt
$NiFeP_{(p.)}$	Potentiostatically modified NiFeP-carbon felt
YP_{fru}	Yeast extract-peptone-fructose

Introduction

Biofuel cells, more popularly known as microbial fuel cells (MFCs), are recently gaining an increasing attention as opportunity for simultaneous electricity generation and waste water purification [1–3]. The low electrical output achieved, however, is the major drawback for their practical utilization. Among all factors influencing the biofuel cell performance, the improvement of the electron transfer from the microorganisms to the anode is considered to be one of the most important one for increasing its efficiency [1, 4–6]. According to Schröder [4], there are two basic mechanisms of the electron transfer in microbial fuel cells: (i) direct electron transfer (DET), which takes place via a physical contact of the bacterial cell membrane or a membrane organelle with the fuel cell anode, with no diffusional redox

Presented at the second workshop on size-dependent effects in materials for environmental protection and energy application, September 19–21, 2010, Nessebar, Bulgaria.

Y. Hubenova (✉)
Department of Biochemistry and Microbiology, Plovdiv University, 4000 Plovdiv, Bulgaria
e-mail: jolinahubenova@yahoo.com

R. Rashkov · V. Buchvarov
Institute of Physicochemistry, Bulgarian Academy of Sciences, 1113 Sofia, Bulgaria

S. Babanova · M. Mitov
Department of Chemistry, South-West University, 2700 Blagoevgrad, Bulgaria

species being involved in the electron transfer from the cell to the electrode; (ii) mediated electron transfer (MET) with the participation of soluble self-produced primary or secondary metabolites or added artificial redox mediators. Although most of the initial studies on MFCs were performed with exogenous mediators, mediatorless biofuel cell systems are presently preferable [7]. It has to be mentioned that the term "mediatorless" means "without artificial mediator of electron transfer" and does not concern the cases when the microbial cultures produce endogenous mediators. On the one hand, the addition of artificial mediators raises the cost of the whole system, and on the other hand, at concentrations high enough for increasing the biofuel cells outputs they could be toxic toward the living cells. In regards to this, different electrode modifications seem to be one of the main approaches for improvement of the MFC performance. The commonly used carbon materials, such as felt, cloth, graphite, etc., possess relatively small electrocatalytic activity toward the bio-anode reactions. The anode performance has been improved by modifications with Mn(IV), Fe(III), Pt, tungsten carbide, polyaniline/Pt composites, covalently linked mediators [8, 9]. However, problems connected with the chemical and the electrochemical stability as well as the biocompatibility of the examined electrocatalysts are hindrances for their wide utilization.

The most reported MFC studies have focused prokaryotic strains used as biocatalysts [1–9]. Reports on the use of eukaryotic cells in MFCs are still rare in the literature. Yeast-biofuel cell research was performed mostly with *Saccharomyces cerevisiae* [10–13]. However, it has been established that *S. cerevisiae* is not an ideal microorganism, as it operates in fermentative/respiration mode with the ratio of fermentation to respiration approximately 80:20 [14]. Thus, the most of the substrate energy remains in the end product of the fermentative pathway. Haslett et al. [14] have recently demonstrated that *Arxula adeninivorans* MFC generates a higher power output than *S. cerevisiae* MFC and this difference is due to the production of an extracellular redox molecule by *A. adeninivorans*. Prasad et al. [15] reported that a mediatorless yeast fuel cell achieved a maximum power density of 2.9 W/m^3 using *Hansenula anomala* as a biocatalyst.

In our recent study [16], a significant improvement of mediatorless yeast-biofuel cell output was achieved using nanomodified Ni-carbon felt anodes and the electrogenic strain *Candida melibiosica 2491* [17]. We have ascertained that this yeast strain accomplishes the electron transfer to the anode combining two mechanisms—by expression of cellular endogenously generated mediator(s) and by formation of yeast biofilm on the modified as well as non-modified carbon felt electrode surface [16]. The supposition that the yeast cells are able to adapt their metabolism and the mechanisms of electron transfer to changes in the anode potential to maximize the biological energy gain is in consensus with other studies concerning anode-respiring cultures [18–20]. Furthermore, modifications with proper metal nanocomposites could adjust the anode potential to desired values that enable better capturing of electron flow from different catabolic steps of living cells, thus increasing the MFC electrical output, or could force the switching over of adaptive cellular response mechanisms connected with the metal ions presence in the surrounding.

Ni–Fe-metal clusters are crucial for the energy production in many bacteria and archaea as they serve as cofactors or prosthetic groups of [NiFe]-hydrogenases [21–26]. Although the hydrogenases activity is proven for bacteria and fungi, the [NiFe]-hydrogenases presence is not well established for yeasts. The intracellular transmembrane transport of iron in yeast cells, however, appears to play an important role. It is supposed that yeasts take up iron by different mechanisms including a formation of metalloprotein complexes like flavo-hemoproteins and siderophore-mediated mechanism with a participation of metal chelators excreted by the cells and attached as ligands to cellular high-affinity receptors [27, 28].

The aim of this study is to develop methods for electrodeposition of nickel–iron and nickel–iron–phosphorus island structures on carbon felt and to examine the performance of the prepared nanomodified materials as anodes in mediatorless yeast-biofuel cell. For this purpose, the biocompatibility of the newly synthesized materials toward *Candida melibiosica 2491* was analyzed and their electrocatalytic properties in MFC were investigated by means of polarization measurements as well as cyclic voltammetry (CV) studies.

Experimental

Electrodeposition and characterization of NiFe and NiFeP nanostructures

Nickel–iron and nickel–iron-phosphorous nanostructures were electrodeposited on carbon felt (SPC-7011, 30 g/m^2, Weißgerber GmbH & Co. KG) by applying galvanostatic or potentiostatic pulse plating technique [16]. The content of the used electrolytes is presented in Table 1. The electrolysis was carried out in a conventional three-electrode cell with platinum–titanium mesh counter electrode and saturated calomel electrode (SCE) as a reference using Gamry G750 potentiostat–galvanostat (Gamry Instruments, US). The electroplating bath temperature was kept constant at 50 °C by thermostat. The characteristics of the applied galvanostatic and potentiostatic pulse regimes are summarized in Table 2.

Table 1 Content of the electrolytes used for electrodeposition of NiFe and NiFeP nanostructures on carbon felt

Electrolyte component	NiFe	NiFeP
$NiSO_4 \cdot 6H_2O$ (g/L)	40	40
$NiCl_2 \cdot 6H_2O$ (g/L)	40	40
$FeSO_4 \cdot 7H_2O$ (g/L)	30	30
H_3PO_4—50% mL	–	11
$Na_2H_2PO_2$ (g/L)	–	4
β-alanine	26	26
Glycine	26	26

Table 2 Regimes applied for electrodeposition of NiFe and NiFeP nanostructures on carbon felt

Regime	I pulse	II pulse	Repetitions
Galvanostatic	100 mA/3 s	Pause/3 s	40
Potentiostatic	−2.2 V(vs. SCE)/ 2 s	−0.3 V(vs. SCE)/ 2 s	40

Scanning electron microscopy (SEM) using Leo 1455VP and Leo Supra 55VP microscopes with energy dispersion X-ray (EDX, Oxford Inca 200 instrument, Software INCA-Vers.4) was applied for characterization of the surface morphology and elemental analysis of the modified carbon felt materials.

Prior to use in MFC, the corrosion behavior of the produced nanomodified materials in neutral medium (67 mM phosphate buffer, pH 7) was investigated by means of potentiodynamic anodic polarization as well as cyclic voltammetry with a scan rate 2 mV/s. The stability of materials was evaluated by estimation of the corresponding corrosion rates from Tafel plots, obtained by potentiodynamic measurements.

Cell cultivation and cytotoxicity test

Yeast strain *Candida melibiosica 2491* was cultivated as previously described [16]. The comparison of the yeast cell growth observed at normal cultivation conditions (YP_{fru} medium, 28 °C) and in the presence of modified carbon felt or addition of Ni^{2+} and Fe^{2+} in concentrations, corresponding to the maximal quantity of the electrodeposited nickel and iron on carbon felt, was used to analyze the potential toxicity of the used new materials. For that purpose the produced nanomodified carbon felt materials were put in a contact with the yeast suspension and the cell development was followed up by measuring the optical density OD600 with time. The same analyses were carried out with addition of Ni^{2+} and Fe^{2+} to the cell suspension in concentrations up to 100 and 50 nmol/L, respectively.

Yeast-biofuel cell studies

The electrocatalytic effects of the deposited nanostructures were investigated by applying the modified carbon felt materials as anodes in double-chamber mediatorless yeast-biofuel cell [16]. A non-modified carbon felt was used as cathode. Both electrodes were fixed in plastic holders, which assured a constant electrode area of 4.5 cm^2 exposed to the electrolyte. Unified quantity of yeast concentrate, corresponding to 0.3 g/L yeast cells, was used as inoculum for biofuel cell experiments. Buffered suspension of *Candida melibiosica 2491* yeast cells in YP_{fru} medium (pH 7) was used as an anolyte and 0.1 M potassium ferricyanide served as a catholyte as well as a final electron acceptor. The anodic and cathodic chambers, each with a volume 13 cm^3, were separated by proton-exchange membrane (Nafion 117, Du Pont).

Polarization measurements at variable resistances (from 100 kΩ to 10 Ω) were carried out at each 6 h using resistance decade box. The load resistances were changed through 2 units at each decade. The cell voltage, U, was recorded 5 min after switching a given resistance by using digital multimeter DMM2700 (Keithley Instruments Inc., US). The current density, i, was calculated in respect to the geometric electrode area using Ohm's law. Polarization curves, presenting the MFC performance, were plotted as U versus i. Power density, P, was estimated for each pair voltage–current density using Joule's law $P = U \times i$ and the corresponding power curves P vs. i were also drawn.

The capability of the yeast-MFC for continuous electricity generation was investigated by switching a load resistance (1 kΩ) in the external electric circuit and monitoring the MFC voltage as well as anode and cathode potentials with time. During these experiments, the anolyte was refreshed at each 24 h by half-replacement with a fresh yeast-free YP_{fru}-medium.

Cyclic voltammetry studies

In order to examine the electron transfer interactions between the yeast cells and the anode, CV-studies of modified electrodes in yeast/YP_{fru}-suspension was carried out at times corresponding to polarization measurements. As a control, CV-measurements of modified carbon felt samples in YP_{fru} medium without yeast cells were also performed. CV-experiments were carried out in three-electrode cell by using PJT 35-2 potentiostat–galvanostat (Radiometer-Tacussel) with IMT 101 electrochemical interface and VoltaMaster 2 data acquisition system. The working electrode potentials were measured against Ag/AgCl reference. Scan rate of 2 mV/s was applied.

Iron-chelating properties of yeast suspension

Yeast suspension at 24th hour of the cells' development was centrifuged at 5000×*g* for 10 min, the collected supernatant was filtered through 0.2 μm sterile syringe filter, and the presence of ferric ions chelator in it was analyzed by means of modified absorption spectrometry method [29]. 0.1 mL $FeCl_3$ (up to 3 mM) was added to 4.9 mL of the sample (100× diluted) and mixed with 5 mL 10 mM KSCN. The absorbance of the obtained red-colored complex was measured at 450 nm using Agilent 8453 UV–VIS–NIR spectrophotometer. The concentration of the residuum free iron was estimated by calibration curve.

All experiments were performed in a minimum of triplicate.

Results and discussion

The morphology of the produced NiFe and NiFeP electrodeposits is shown in Fig. 1. As seen from the SEM-images, globular island-structure deposits with particle sizes from 100 to 500 nm have been obtained by both regimes applied. As a whole, the prepared nanoparticles are larger than previously studied nickel island nanostructures [16]. The phosphorous content above 10 wt% leads to amorphization of the produced composites [30], which may explain the more uniform rounded shape of the NiFeP particles in comparison with the microcrystalline NiFe ones. However, under potentiostatic mode applied, the observed anodic current during the second pulse (−0.3 V vs. SCE) is connected with a partial dissolution of the deposits' surface, which results in rougher and more developed surface of the particles in these cases.

Table 3 Elemental content of the electrodeposited island nanostructures

Electrodeposit	Regime	Ni (wt%)	Fe (wt%)	P (wt%)	O (wt%)
NiFe	Potentiostatic	55	29	–	16
	Galvanostatic	62	30	–	8
NiFeP	Potentiostatic	75	6	13	6
	Galvanostatic	71	9	13	7

The elemental analysis, obtained by EDX, shows that the component content is almost independent of the type of the applied pulse plating technique. The ratio Ni:Fe is approximately 2:1 in the NiFe electrodeposits, while the presence of phosphorus results in augmentation of Ni and decrease of Fe content (Table 3).

The electrochemical performance of the produced nanomodified NiFe- and NiFeP-carbon felt materials in neutral medium (phosphate buffer, pH 7) is presented in Fig. 2. Identical CV patterns were obtained with electrodes with the same elemental content but produced under different pulse plating regimes (see Table 3). That is why only

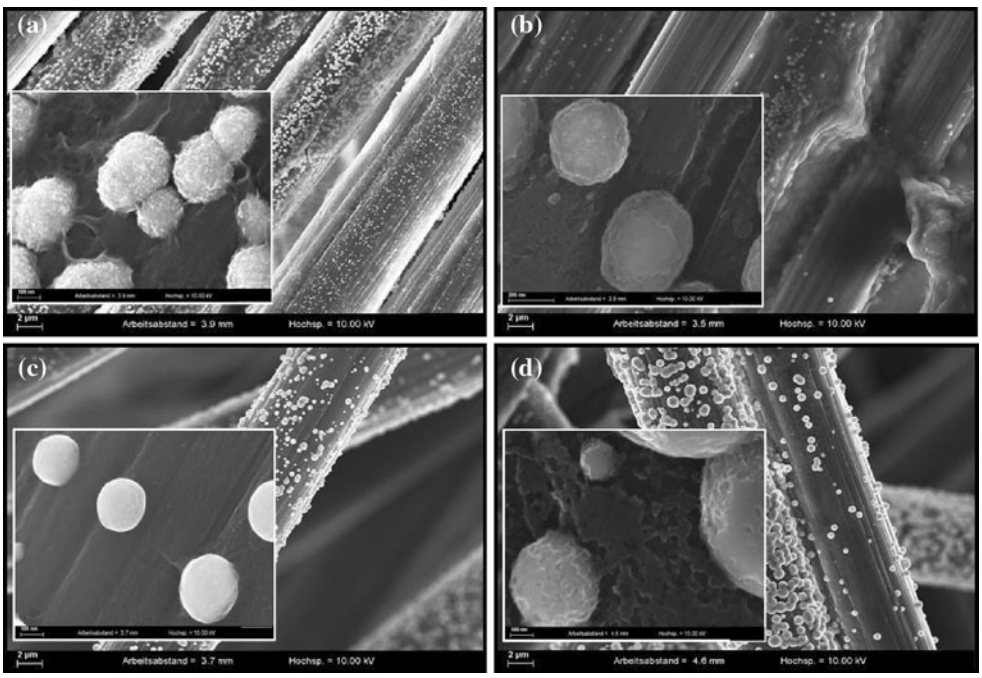

Fig. 1 SEM images of: **a** NiFe-modified carbon felt obtained under multiple galvanostatic pulse; **b** NiFe-modified carbon felt obtained under multiple potentiostatic pulse; **c** NiFeP-modified carbon felt obtained under multiple galvanostatic pulse; and **d** NiFeP-modified carbon felt obtained under multiple potentiostatic pulse conditions

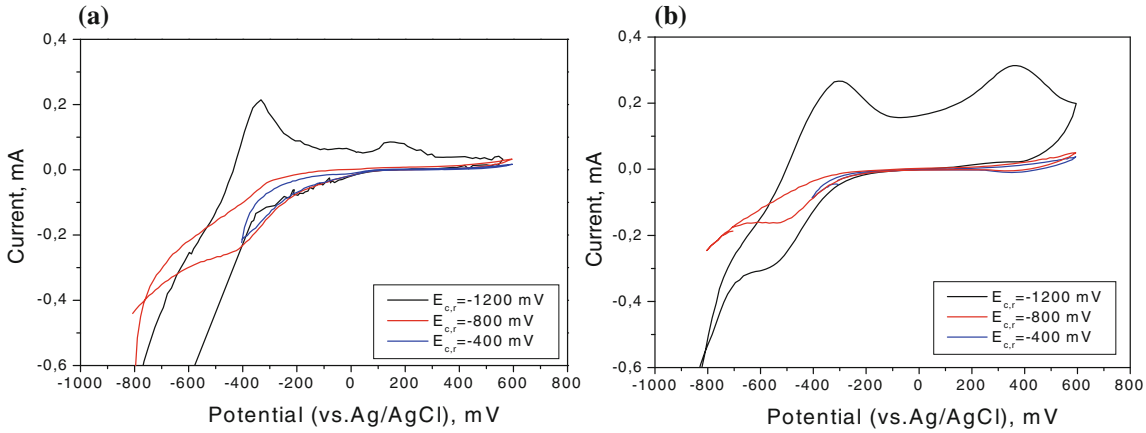

Fig. 2 Cyclic voltammograms obtained with: **a** NiFe-carbon felt; **b** NiFeP-carbon felt electrodes in phosphate buffer (pH 7); scan rate 2 mV/s

Table 4 Corrosion potentials, E_{corr}, and currents, I_{corr}, of the studied electrodes in neutral phosphate buffer

Electrodeposit	E_{corr}, mV (vs. Ag/AgCl)	I_{corr} (μA)
NME (C-felt)	−279 ± 25	11.1 ± 4.6
NiFe(p.)	−126 ± 15	10.0 ± 3.9
NiFe(g.)	−121 ± 9	8.4 ± 3.7
NiFeP(p.)	−166 ± 16	7.2 ± 2.6
NiFeP(g.)	−140 ± 19	11.3 ± 3.6

one cyclic voltammogram is shown for each type (NiFe- and NiFeP-) of modified electrodes. When the potential was swept in the range between −400 and +600 mV versus Ag/AgCl no peaks appeared in the recorded voltammograms, while if the cathodic scan was performed up to −1200 mV, two broad anodic peaks related to electro-oxidation of the metals to different oxidation states appeared in the reverse anodic scan. The observed behavior is connected with the existence of protective surface coatings on the electrodeposited nanoparticles, which are reduced by the evolved hydrogen only when the cathodic switch potential is negative enough.

The corrosion rates and potentials of each material were estimated from Tafel plots, obtained by potentiodynamic anodic polarization, are presented in Table 4.

As seen from the data, the corrosion rates of all modified materials are close or even smaller than that of non-modified carbon felt electrodes (NME). In addition, the shift of E_{corr} to more positive values reveals a lower affinity to corrosion of the produced nanomodified electrodes in comparison with the bare carbon felt.

The spectrophotometric measurements of OD600 in the progress of *Candida melibiosica 2491* yeast strain cultivation show that the culture development is not inhibited by the presence of the examined modified materials. The analyses for cytotoxicity performed with addition of Ni and

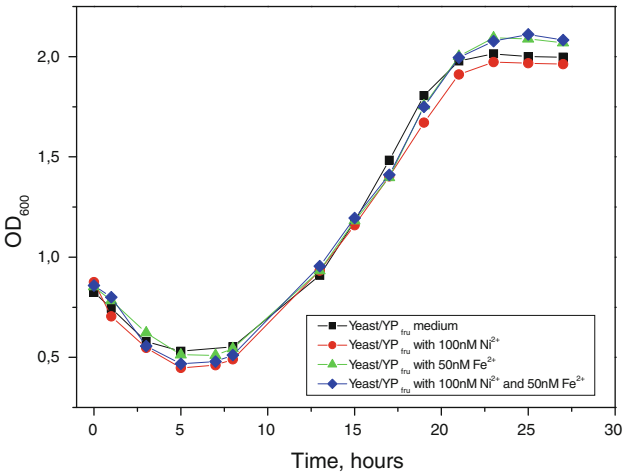

Fig. 3 Development of *Candida melibiosica* in YP_{fru} medium in the absence (*squares*) and presence of metal ions: Ni^{2+} (*circles*); Fe^{2+} (*triangles*); Ni^{2+}: Fe^{2+} = 2:1 (*rhombuses*)

Fe ions to the growth medium, in concentrations equivalent to the maximal amounts of the metals in the produced electrodeposits, also confirmed that these metal ions do not disturb the cell development and it is commensurable to the growth of the control (Yeast/YP_{fru}) (Fig. 3). The presented graphs describe well-defined lag-, exponential-, and stationary phases of the yeast development. The observed deviations from the control in the presence of heavy metals during the lag-phase could be explained with a switching on of adaptive mechanisms of the yeast cells connected with (i) increased expression of molecules taking part in the bringing the Ni- and Fe-ions into the cells for their further participation as prosthetic groups of the important for the cell energy system [NiFe]-hydrogenases [27] or (ii) restriction of metal entry into the cells [31]. Summarizing the results from the conducted cytotoxicity tests we have concluded that the prepared nanomodified carbon felt materials are non-toxic toward *Candida melibiosica 2491*

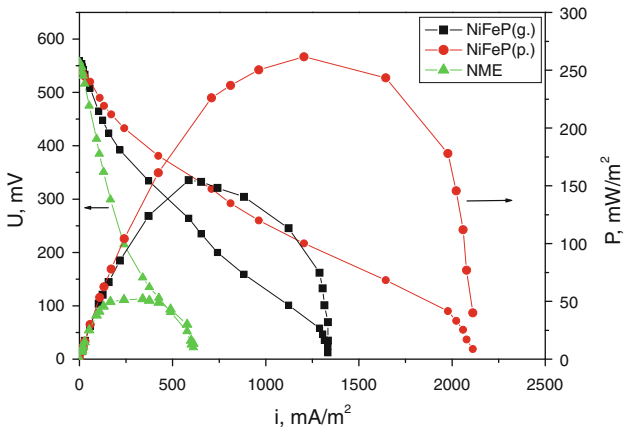

Fig. 4 Polarization and power curves obtained with *Candida melibiosica* yeast-biofuel cell with $NiFeP_{(g.)}$ (*squares*), $NiFeP_{(p.)}$ (*circles*), and NME (*triangles*) anodes

yeast cells and could be applied as electrodes in yeast-biofuel cell.

The application of the produced modified materials as anodes in mediatorless yeast-biofuel cell has shown that all of them increase the MFC outputs in comparison with the use of non-modified electrodes (NME). Higher maximum power density values have been achieved with NiFeP-carbon felt anodes—260 ± 8 and 155 ± 6 mW/m^2 with potentiostatically ($NiFeP_{(p.)}$) and galvanostatically ($NiFeP_{(g.)}$) modified ones, respectively, against 52 ± 9 mW/m^2 for the NME (Fig. 4). Lower power density, exceeding just 1.8 and 1.6 times that of the control has been obtained with $NiFe_{(p.)}$ and $NiFe_{(g.)}$ anodes. For the latter, an increase of the MFC outputs was attained using $KMnO_4$ instead of $K_3[Fe(CN)_6]$ as a catholyte, however, the permanganate reduction produced insoluble manganese dioxide which precipitated on the cathode, thus impeding its proper operation. It is worth noting that the highest outputs with the investigated modified electrodes were achieved in the earlier stage (12th to 18th h) than with NME and previously reported Ni-nanomodified ones [16]. This indirectly indicates that the presence of NiFe and NiFeP nanocomposite structures modulates the yeast cells to switch on metabolic mechanisms responsible for the observed electrochemical activity at earlier stages of the yeast culture development. In summary, comparing the results from this and our previous study [16], the increase of the iron content in the electrodeposited nanostructures tends toward a decrease in the yeast-MFC current and power outputs when the corresponding modified materials were used as bioanodes. One of the possible explanations of the discussed performance may be connected with the increasing specific resistance of modified materials with the enrichment of iron in the deposited nanocomposite structures, resulting in the observed increase of the internal cell resistance. Another possible reason could be assigned to the individual electrocatalytic properties of the different modified materials, including their intrinsic catalytic activity, which depends on the particular elemental content and distribution of the electrodeposited nanostructures, as well as the specific surface area, influenced on the particle size and morphology of the produced materials. The better performance achieved with potentiostatically deposited NiFeP and NiFe anodes in comparison with the corresponding ones obtained by galvanostatic pulse plating technique is most probably connected with the more developed particles' surface of the former due to the partial anodic dissolution during electrodeposition. Besides the different elemental content, the lower electrocatalytic activity of the examined modified materials in comparison with that of previously studied Ni-nanomodified carbon felt [16] may be assigned to the quite smaller size of the Ni particles, which results in a larger surface area of the latter materials. The last but not least reason for the observed behavior, however, may be associated with specific metabolic mechanisms switched on by the yeast cells as a response to the different metallic content in the environment.

In a batch mode, a drop in the MFC-outputs after 24 h operation was observed. In order to overcome that we performed experiments in a fed-batch mode, in which a half of the yeast suspension was periodically replaced with fresh YP_{fru} medium. In these experiments, the MFC was continuously loaded with an external resistance and the terminal voltage, anodic, and cathodic potentials were simultaneously monitored. The obtained results are illustrated in Fig. 5. The plotted discharge curves show that the MFC-voltage, respectively, current output, is mainly determined by variations of the anodic potential, while the cathodic potential becomes almost steady-state after an initial drop in the first 24 h. Therefore, the whole MFC-performance is limited by

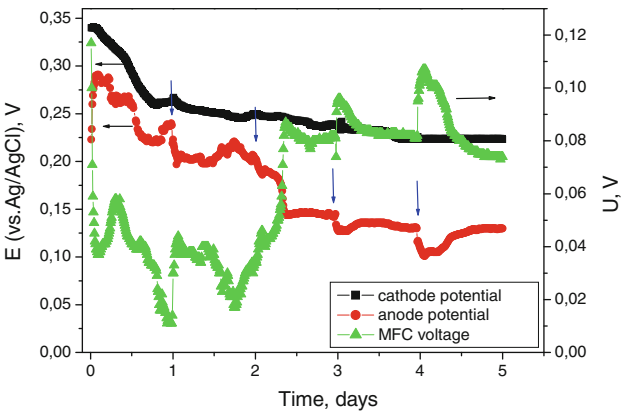

Fig. 5 Variation of voltage (*triangles*), anode (*circles*), and cathode (*squares*) potential of MFC with modified NiFeP-carbon felt anode and non-modified carbon felt cathode, operating in a fed-batch mode. The *vertical arrows* indicate the refreshment of the anolyte

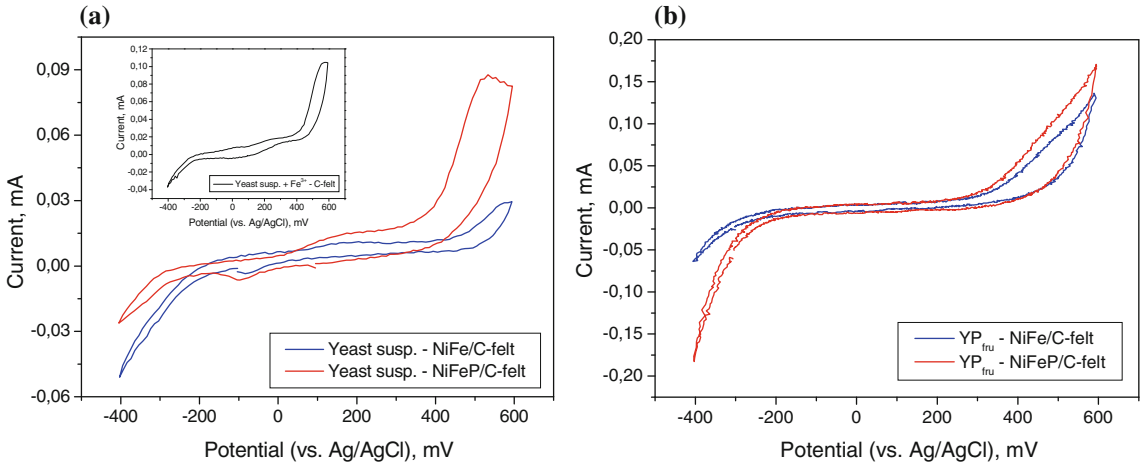

Fig. 6 Cyclic voltammograms obtained with NiFe-carbon felt and NiFeP-carbon felt electrodes in: **a** *Candida melibiosica* yeast/YP$_{fru}$ suspension, inner graph—NME in yeast suspension with addition of Fe^{3+}; **b** YP$_{fru}$ medium without yeast cells; scan rate 2 mV/s

the anode-half reaction connected with the electron transfer interactions between the yeast cells and the bioanode. Each refreshment of the yeast suspension led to a shift of the anodic potential in negative direction, respectively, increase of the biofuel cell voltage. Relatively stable MFC-characteristics were achieved after the second refreshment of the anolyte, which is probably associated with the previously reported biofilm formation [16].

In order to elucidate the origin of the observed electrochemical activity, cyclic voltammetry study with the modified carbon felt electrodes in yeast suspension as well as in YP$_{fru}$ medium without yeast cells was carried out. Cyclic voltammograms recorded at times relevant to the optimum MFC characteristics achieved are presented in Fig. 6.

In contrary to the previously studied nanomodified Ni-carbon felt, the CV performance of NiFe- and NiFeP-carbon felt electrodes in yeast/YP$_{fru}$ suspension (Fig. 6a) looks like that of non-modified ones, characterized by separated anodic and cathodic peaks connected with a production of endogenous electron shuttle during the mid-log phase of yeast growth [16]. However, the observed anodic and cathodic peak at +175 and −100 mV vs. Ag/AgCl, respectively, are shifted about 50 mV in the negative direction when compared with those obtained with non-modified carbon felt (inner graph), which indicates a facilitated electron transfer from the yeast suspension to the modified electrode surface. The absence of the aforementioned peaks in the voltammograms obtained with fresh YP$_{fru}$ medium non-inoculated with yeast cells (Fig. 6b) proves that their origin is connected with bioelectrocatalytic effect, and not with a direct electrooxidation/reduction of substances in the medium or corrosion of the electrodes. The characteristic peaks obtained with NiFeP electrodes are more intensive than those with NiFe ones, which correlates with their performance as anodes in MFC. The broad anodic peak at potentials over +500 mV, more expressed in the voltammograms obtained with NiFeP modified electrodes, should not be associated with the reactions that take place on the MFC bioanode, because its potential is rather positive than the anodic potentials recorded during biofuel cell polarization measurements. The origin of this peak may be assigned to oxidation of either the electrode material itself or not readily oxidizable species, presented in the electrolyte. The position of the peaks corresponding to a formation of metallic ions in higher oxidation state (Fig. 2), however, does not coincide with the potential of the intensive anodic peak in voltammograms obtained in yeast suspension (Fig. 6a). Thus, it can be concluded that the latter is not connected with a corrosive oxidation of the electrodeposited nanocomposites. Furthermore, CV pattern similar to those with modified electrodes was obtained when Fe^{3+} ions were added to the yeast suspension and cyclic voltammetry was carried out with non-modified carbon felt working electrode (Fig. 6a, inner graph). Taking into account this we supposed that the observed intensive anodic peak is more probably associated with a formation of highly stable extracellular ferric complexes, like siderophores, as a response to the yeast iron uptake mechanism [27].

To examine such a hypothesis, determined amounts of ferric ions were added to a supernatant, obtained by centrifugation of yeast suspension at times corresponding to its highest electrochemical activity, and the quantity of strongly bonded iron was estimated as a difference between the introduced and the residuum free iron in the medium, determined by means of spectrophotometric analysis (Table 5). The significant decrease of Fe^{3+} concentration in the supernatant samples indicates that part of them is bounded with a soluble component of the yeast suspension

Table 5 Concentration of chelated Fe^{3+} (Δc) in the supernatant of fractionated yeast anolyte suspension; control—deionised water

Sample	Fe^{3+} introduced (mmol/L)	Fe^{3+} determined (mmol/L)	Δc (Fe^{3+}) (mmol/L)
Control	2.00	1.82 ± 0.08	0.18 ± 0.08
Supernatant		1.09 ± 0.05	0.91 ± 0.05
Control	2.40	2.26 ± 0.07	0.14 ± 0.07
Supernatant		1.14 ± 0.07	1.26 ± 0.07
Control	3.00	2.91 ± 0.06	0.09 ± 0.06
Supernatant		1.86 ± 0.03	1.14 ± 0.03

in a more stable complex than the analyzable $[Fe(SCN)]^{2+}$ one, i.e., proves the presence of strong ferric iron chelator.

Conclusions

The application of nanomodified NiFe- and NiFeP-carbon felt, produced by electrodeposition, as anodes in mediatorless yeast-biofuel cell results in an improvement of its electrical outputs. The observed electrocatalytic activity of the studied materials depends on their elemental content, but also on the preparation technique applied. The electrode performance improves with an increase of nickel and a decrease of iron content. At the same time, the better performance of potentiostatically over galvanostatically deposited electrodes could be assigned to the more developed particles' surface of the former due to a partial anodic dissolution during preparation. The obtained results in a fed-batch mode reveal potentials for long-term operation of the system.

Acknowledgements This study was funded by the National Science Fund of Bulgaria through contract D002-163/2008 and partially supported by the German Research Society (DFG) within a joint research project between the Institute of Physical Chemistry of the BAS, Bulgaria, and the Research Institute for Noble Metals and Chemistry of Metals, Schwabisch Gmund, Germany. The authors gratefully thank Danail Georgiev from Plovdiv University "Paisii Hilendarski", Plovdiv, Bulgaria; Elitsa Chorbadjijska and Georgi Hristov from South-West University "Neofit Rilsky", Blagoevgrad, Bulgaria for their support during the implementation of the study.

References

1. Du Z, Li H, Gu T (2007) Biotechnol Adv 25:464
2. Rabaey K, Verstraete W (2005) Trends Biotechnol 23:291
3. Bullen RA, Arnot TC, Lakeman JB, Walsh FC (2006) Biosens Bioelectron 21:2015
4. Schröder U (2007) Phys Chem Chem Phys 9:2619
5. Cheng S, Liu H, Logan BE (2006) Environ Sci Technol 40:2426
6. Rabaey K, Boon N, Siciliano SD, Verhaege M, Verstraete W (2004) Appl Environ Microbiol 70:5373
7. Davis F, Higson SPJ (2007) Biosens Bioelectron 22:1224
8. Logan BE, Hamelers B, Rozendal R, Schröder U, Keller J, Freguia S, Aelterman P, Verstraete W, Rabaey K (2006) Environm Sci Technol 40:5181
9. Rinaldi A, Mecheri B, Garavaglia V, Licoccia S, Nardo P, Traversa E (2008) Energy Environ Sci 1:417
10. Chiao M, Lam KB, Lin L (2006) J Micromech Microeng 16:2547
11. Walker AL, Walker CW (2006) J Power Sour 160:123
12. Gunawardena A, Fernando S, To F (2008) Int J Mol Sci 9:1893
13. Ganguli R, Dunn B (2009) Fuel Cells 9:44
14. Haslett ND, Rawson FJ, Barriere FEE, Kunze G, Pasco N, Gooneratne R, Baronian KHR (2010) Characterisation of yeast microbial fuel cell with the yeast Arxula adeninivorans as the biocatalyst. Biosens Bioelectron doi:10.1016/j.bios.2011.02.011
15. Prasad D, Arun S, Murugesan M, Padmanaban S, Satyanarayanan RS, Berchmans S, Yegnaraman V (2007) Biosens Bioelectron 22:2604
16. Hubenova Y, Rashkov R, Buchvarov V, Arnaudova M, Babanova S, Mitov M (2010) Improvement of yeast-biofuel cell output by electrode modifications. Ind Eng Chem Res. doi:10.1021/ie1000949
17. Hubenova Y, Mitov M (2010) Bioelectroch 78:57
18. Lovley DR, Giovannoni SJ, White DC, Champine JE, Phillips EJP, Gorby YA, Goodwin S (1993) Arch Microbiol 159:336
19. Kim BH, Kim HJ, Hyun MS, Park DH (1999) J Microbiol Biotechn 9:127
20. Bond DR, Lovely DR (2003) Appl Environ Microbiol 69:1548
21. Barton BE, Whaley CM, Rauchfuss TB, Gray DL (2009) J Am Chem Soc 131:6942
22. Loescher S, Burgdorf T, Buhrke T, Friedrich B, Dau H, Haumann M (2005) Biochem Soc Trans 33:25
23. Vignais PM, Colbeau A (2004) Curr Issues Mol Biol 6:159
24. Garcin E, Vernede X, Hatchikian EC, Volbeda A, Frey M, Fontecilla-Camps JC (1999) Structure 7:557
25. Albracht SPJ (1994) BBA 1188:167
26. Teixeira VH, Baptista AM, Soares CM (2006) Biophys J 91:2035
27. Blaiseau PL, Seguin A, Camadro JM, Lesuisse E (2010) In: Cornelis P, Andrews SC (eds) Iron uptake and homeostasis in microorganisms. Caister Academic Press, Norfolk
28. Neilands JB (1995) J Biol Chem 270:26723
29. Dobrinas S, Soceanu A, Gheorghiu CB, Tanase M (2010) Ovidius Univ Ann Chem 21:35
30. Sridharan K, Sheppard K (1997) J Mater Process Technol 68:109
31. Fomina M, Burford E, Gadd G (2005) In: Dighton J, White JF, Oudemans P (eds) The fungal community: its organization and role in the ecosystem. CRC Press, Boca Raton